forests

MDPI

Article

The Potential Distribution Prediction of the Forestry Pest *Cyrtotrachelus buqueti* (Guer) Based on the MaxEnt Model across China

Chun Fu [1,†], Zhiling Wang [2,†], Yaqin Peng [2] and Zhihang Zhuo [2,*]

[1] Key Laboratory of Sichuan Province for Bamboo Pests Control and Resource Development, Leshan Normal University, Leshan 614000, China; fuchun19841005@lsnu.edu.cn
[2] College of Life Science, China West Normal University, Nanchong 637002, China; wangzhiling995@foxmail.com (Z.W.); pengyaqin2023@foxmail.com (Y.P.)
* Correspondence: zhuozhihang@cwnu.edu.cn; Tel.: +86-1311-197-3927
† These authors contributed equally to this work.

Abstract: Exploring the geographical distribution of forestry pests is crucial for formulating pest management strategies. *Cyrtotrachelus buqueti* (Guer) stands out as one of the primary pests among China's forestry hazards. This study employs the MaxEnt model, along with 19 bioclimatic variables and habitat characteristics, to predict the current and future distribution of *C. buqueti* under three typical emission scenarios for 2050 and 2070 (2.6 W/m^2 (SSP1-2.6), 7.0 W/m^2 (SSP3-7.0), and 8.5 W/m^2 (SSP5-8.5)). Among the 19 bioclimatic variables, BIO 14 (precipitation of the driest month), BIO 8 (mean temperature of the wettest quarter), Elev, slope, and aspect were identified as significant contributors. These five variables are critical environmental factors affecting the suitability of habitats for *C. buqueti* and are representative of its potential habitat. The results indicate that *C. buqueti* predominantly inhabits southern regions such as Chongqing, Guizhou, Yunnan, Sichuan, Guangxi, Shaanxi, Hubei, Hainan, and Taiwan. Among them, Chongqing, Guizhou, and Yunnan are the primary distribution areas of high suitability. In the future, the centroid's movement direction will generally shift southward, with an expansion trend observed in the distribution areas of each province. This study enhances researchers' understanding of forestry pest dynamics and promotes proactive management strategies to mitigate their impact on forest ecosystems and agricultural productivity.

Keywords: *Cyrtotrachelus buqueti*; forestry nuisance species; potential distribution; MaxEnt model; future climate scenarios

Citation: Fu, C.; Wang, Z.; Peng, Y.; Zhuo, Z. The Potential Distribution Prediction of the Forestry Pest *Cyrtotrachelus buqueti* (Guer) Based on the MaxEnt Model across China. *Forests* **2024**, *15*, 1049. https://doi.org/10.3390/f15061049

Academic Editor: Viacheslav I. Kharuk

Received: 8 April 2024
Revised: 13 May 2024
Accepted: 13 June 2024
Published: 18 June 2024

1. Introduction

Cyrtotrachelus buqueti (Guer) (Coleoptera: Curculionidae), also known as the bamboo snout beetle, belongs to the Cyrtotrachelus family, Curculionoidea superfamily, and Coleoptera order. It is widely distributed in Southeast Asian countries such as China, Vietnam, Myanmar, and Thailand [1,2]. In April 2003, *C. buqueti* was included in the List of Forest Pests of China [3]. This pest mainly damages plants in the bamboo subfamily and is currently one of the most significant pests in bamboo forests. Its damage rate to dense bamboo forests can range from 50% to 90% [4]. As a notable forestry pest, *C. buqueti* has become a key limiting factor in the development of bamboo forests for papermaking, resulting in significant economic losses and impacting ecological development [2,5]. Currently, the survival of 28 different types of bamboo is threatened by it, especially in the *Bambusa*, *Dendrocalamopsis*, and *Dendrocalamus* genera. The surface of the leaves that have been attacked by it shows irregularly shaped bite marks of varying sizes, and sometimes, the entire leaf is consumed, resulting in extensive damage. This can also lead to the formation of brown or black spots at the damaged areas on the leaves, caused by the oxidation of

the tissues after being damaged. The larvae of *C. buqueti* show a greater preference for bamboo during the bamboo shoot period [6], particularly targeting *Phyllostachys edulis* (Carrière) J. Houz., *Dendrocalamopsis oldhami* (Munro) Keng f., *Bambusa textilis* McClure, *Bambusa pervariabilis* McClure, *Bambusa grandis* (Q. H. Dai & X. L. Tao) Ohrnb., and other sympodial bamboo species [7]. However, in areas of food scarcity, the larvae may also feed on other clumping bamboos such as *Neosinocalamus affinis* and *Bambusa textilis* [4,8]. Before burrowing into the soil, the larvae of *C. buqueti* primarily inhabit the concealed shoots, which is one of the reasons that they tend to feed on bamboo shoots [9]. Interestingly, *C. buqueti* requires only about 20 days of feeding during its larval stage to sustain its energy needs throughout its entire lifespan [10]. Subsequently, during the mature larval stage, *C. buqueti* burrows underground, undergoing three developmental stages—mature larva, pupa, and adult—before emerging as an adult the following year. Upon emergence, the adults concentrate their activities, such as feeding, mating, and egg-laying, at the tips of bamboo shoots [11,12]. *C. buqueti* belongs to the Coleoptera order, a group of insects characterized by having thick and hard forewings. This feature allows them to greatly reduce abdominal movement during flight, thereby reducing energy consumption. At the same time, *C. buqueti* possesses soft hindwings. While crawling on the ground, they can fold them and tuck them under their hard forewings, serving as a protective measure. Particularly notable is the intricate venation structure of the hindwings, allowing them to fully expand during flight and achieve joint self-locking [13]. This structure enables them to control yaw direction during flight, allowing for agile movement within dense bamboo forests [14]. In addition, the proboscis of *C. buqueti* also possesses powerful drilling capabilities. This is attributed to its proboscis being a rigid keratinous structure, endowed with excellent mechanical properties such as high specific strength and stiffness [15,16]. The ability of this pest to survive in hard and dense bamboo forests is precisely due to these morphological features.

Bamboos belong to the Bambusoideae subfamily within the Poaceae family. This plant is a natural organic polymer material [17,18], playing a significant role in ecology, economy, and culture worldwide, especially in the tropical regions of Asia, the Americas, and Africa [19]. The utility of bamboos is further evidenced by their wide range of applications, rapid growth, and potential for sustainable harvesting [20]. Bamboo is known to have over 4000 traditional uses and over 1500 commercial applications. For instance, it is utilized as fuel and in the construction of furniture materials [21]. In particular, in Southeast Asian countries, bamboo has a long history of being used as construction and furniture materials [17]. Due to its fast growth rate and sustainable harvesting characteristics, bamboo has become an alternative source of industrial fibers and renewable energy [22]. Furthermore, research indicates that bamboo also plays a role in restoring soil fertility [23–25]. The aforementioned utilization of bamboo primarily relies on its woody cellulose fibers, which are important biomass resources [26]. It is noteworthy that *C. buqueti* primarily causes damage to bamboo through its degrading effect on its woody cellulose fibers [10]. Furthermore, research suggests that *C. buqueti* is capable of degrading bamboo woody cellulose both internally and externally [26]. Due to the fact that both larvae and adults primarily feed on bamboo shoots, which are rich in woody cellulose fibers, research speculates that *C. buqueti* utilizes bamboo woody cellulose for its growth and development [27]. Compared to other types of bamboo, clumping bamboo has unique development value. Clumping bamboo refers to bamboo plants that grow in clusters or dense stands. These bamboos typically grow closely together in dense groves or communities, with their stems closely spaced, forming thickets of bamboo. Its difference lies in the absence of an extensive rhizome system; thus, it does not expand its growing area extensively, making it easier to manage [28]. However, *C. buqueti* exhibits a distinct preference for this uniquely valuable clumping bamboo, posing a significant threat. Therefore, prevention and control efforts for *C. buqueti* merit a multifaceted approach. Conventional control methods primarily involve chemical, physical, and biological measures, all of which are reactive measures implemented in

areas already affected by infestation. However, this study focuses on predicting areas susceptible to infestation due to climate change. It offers preventive measures for regions that may face infestation in the future.

Species distribution models (SDMs), also known as environmental niche models, are primarily used to determine the presence or absence of target species within a specific area. These models also aim to predict and assess the spatial distribution and redistribution of species under environmental changes [29]. Furthermore, it can utilize observed distribution data to deduce the ecological preferences of species and create maps to illustrate their potential distribution. The application scope of SDMs spans from studying the impacts of human activities on climate change to predicting biological invasions. It is typically created by associating known species occurrence (or presence–absence) data with information about environmental conditions at these locations [30]. SDMs rely on available occurrence records to explore the relationship between observed species presence and potential environmental parameters that directly or indirectly influence species distribution in known areas. It utilizes this information to predict the likelihood of species occurrence in other regions [31]. In this study, to predict the target species, we opted for a highly efficient and extensively employed method in SDMs, namely the maximum entropy model (MaxEnt). MaxEnt is a method that relies on background information and has been successfully applied in multiple fields [32]. It is widely used to address increasingly complex issues across various fields, such as ecology and geography [33], epidemiology [34], conservation biology [35], and invasion biology [36]. However, this paper primarily utilizes MaxEnt for prediction, niche modeling, species forecasting, and habitat suitability assessment. MaxEnt only necessitates widely available presence-only data for preliminary species distribution data [37]. It can generate robust predictive models with a small amount of presence-only data, primarily due to the principles of the model, a powerful technique for estimating the probability model state [38]. In particular, other models may suffer from complexity in operation and modeling. However, the statistical and computational complexity of MaxEnt has been overcome by the practical simplicity of the powerful, platform-independent, and free Java™ tool known as maxent.jar. This significantly lowers the accessibility threshold. The relevant digital ecological data can largely be leveraged, such as the Global Biodiversity Information Facility (GBIF) (https://www.gbif.org, accessed on 3 April 2024), along with various geographic information systems, which can be integrated [39]. Overall, it is characterized by a small sample size, strong operability, and high reliability in predictive performance.

This study employs the MaxEnt model, combined with 19 bioclimatic variables and three terrain factors, to predict the geographical distribution of *C. buqueti* from multiple perspectives. The aim is to explore the future dynamic distribution patterns in areas already affected by infestation, as well as the level of risk in undiscovered regions. Furthermore, key influencing factors are identified based on the prediction results, providing scientific insights from a geographical distribution perspective for the control and prevention of *C. buqueti*.

2. Materials and Methods

2.1. Species Presence Records and Selection Criteria

In total, this study collected 379 occurrence records of *C. buqueti*. These data were primarily obtained from the Global Biodiversity Information Facility (GBIF: https://www.gbif.org, accessed on 3 April 2024) database. In addition to online databases, distribution point data from actual surveys were also retrieved from the relevant literature in the CNKI and Web of Science databases. Occurrence records without precise geographical information were excluded. The remaining occurrence records underwent spatial analysis using the ArcGIS tool to estimate distances between distribution points, ensuring that the straight-line distance between two points was greater than 10 km to identify duplicates, which were subsequently removed. To avoid overfitting, ENMTools v1.3 (https://www.example.com/enmtools, accessed on 20 April 2024) was used to retain only one occurrence record for each 5 × 5 km grid. Finally, 374 occurrence records of *C. buqueti* were selected for modeling using the MaxEnt model.

2.2. Environmental Variables and Selection Criteria

The environmental variables involved a total of 22 variables. They consisted of two parts: three terrain factors and 19 bioclimatic variables (BIO 1–BIO 19) (Table 1). The global elevation (DEM) data were sourced from the National Centers for Environmental Information (NCEI) of the National Oceanic and Atmospheric Administration (NOAA) (https://www.ngdc.noaa.gov/, accessed on 3 April 2024). The 19 bioclimatic variables were obtained from the current and future datasets of the WorldClim global climate database (http://www.worldclim.org/, accessed on 3 April 2024). The current climate data were selected from the period between 1970 and 2000. The future climate data were derived from two time periods: the 2050s (2041–2060) and the 2070s (2061–2080). The future data utilized the second-generation National Climate Center's Medium-Resolution Climate System Model (BCC-CSM2-MR). Regarding the future climate scenario data, three socio-economic pathways, namely SSP1-2.6, SSP3-7.0, and SSP5-8.5, from the Sixth Coupled Model Intercomparison Project (CMIP6), were selected. These pathways represent different levels of greenhouse gas emissions, aiming to simulate the future distribution of the target species, representing minimal-, moderate-, and maximum-emission scenarios [40].

Table 1. Three terrain factors and 19 bioclimatic variables.

Abbreviation	Description
BIO 1	Annual mean temperature (°C)
BIO 2	Mean diurnal range (monthly mean (max temp-min temp)) (°C)
BIO 3	Isothermally (BIO 2/BIO 7) × 100
BIO 4	Temperature seasonality (standard deviation × 100) (C of V)
BIO 5	Max temperature of the warmest month (°C)
BIO 6	Min temperature of the coldest month (°C)
BIO 7	Temperature annual range (BIO 5-BIO 6) (°C)
BIO 8	Mean temperature of the wettest quarter (°C)
BIO 9	Mean temperature of the driest quarter (°C)
BIO 10	Mean temperature of the warmest quarter (°C)
BIO 11	Mean temperature of the coldest quarter (°C)
BIO 12	Annual precipitation (mm)
BIO 13	Precipitation of the wettest month (mm)
BIO 14	Precipitation of the driest month (mm)
BIO 15	Precipitation seasonality (C of V)
BIO 16	Precipitation of the wettest quarter (mm)
BIO 17	Precipitation of the driest quarter (mm)
BIO 18	Precipitation of the warmest quarter (mm)
BIO 19	Precipitation of the coldest quarter (mm)
Elevation (Elev)	Elevation of the terrain
Slope	Slope or obliquity of the terrain
Aspect	The direction or orientation of the earth's surface

Environmental variables form the foundation of niche model modeling, and filtering them enhances the accuracy of the model. The environmental variables discussed in this article represent a general assumption about various conditions. It is essential to identify the key variables that affect the distribution of *C. buqueti* as the species' habitat preferences are not adequately represented. Typically, an increase in regularization gain is used to represent the contribution level of the corresponding variables. The first estimate is determined by first obtaining the increase in regularization gain, which is then added to the contribution of the respective variable. This process is repeated in each iteration of the training algorithm. In one scenario, if there is a negative change in the absolute value of lambda, the variable is removed. The second estimate involves randomly permuting the values of environmental variables on the training set and background data. Based on this, the model is re-evaluated and normalized to percentages, and its importance is assessed. Furthermore, in conjunction

with the jackknife test in the MaxEnt model, the contribution rate of each variable can be obtained. Variables with smaller contributions should be excluded. Pearson correlation coefficients were used to identify highly correlated variables ($|r| \geq 0.8$). To enhance the accuracy of the model and address issues of multicollinearity, variance inflation factor (VIF) analysis was conducted for all 21 variables. Variables with VIF values exceeding 100 were removed. Finally, the remaining environmental factors with VIF values less than 100 and correlations less than 0.8 were used for model prediction.

2.3. Calibration, Construction, and Evaluation of the MaxEnt Model

The optimization of MaxEnt's default settings was an essential step for mitigating potential overfitting. Constructing the MaxEnt model involved adjusting the feature combinations (FCs) and regularization multiplier (RM), which could effectively improve the model's accuracy. The FCs established the relationship between the species and the environment, ranging from simple to highly complex non-linear relationships. It comprised five features: linear (L), quadratic (Q), hinge (H), product (P), and threshold (T). These features were combined in various ways to achieve the optimal combination. After multiple combinations and screenings, the final adjustment to the FC in this study model was LQHP, with an RM of 0.3. The other related settings can be viewed in Table S1. When the difference in delta_AICc between the optimized parameter model and the default parameter model is less than or equal to 2, it indicates a superior performance of the optimized model [41]. Twenty-five percent of the filtered occurrence points were set aside as the test set, while the remaining records were used for training. The maximum number of iterations was set to 500, and the maximum background point number was set to 10,000, with 10 repetitions. The Receiver Operating Characteristic Curve (ROC)'s Area Under the Curve (AUC) was used to evaluate the accuracy of the model results. The AUC value is independent of threshold values in the model and ranges from 0 to 1, where 0 to 0.6 indicates poor predictive performance, 0.7 to 0.8 represents fair predictive performance, 0.8 to 0.9 indicates good predictive performance, and 0.9 to 1.0 represents excellent predictive performance. AUC values greater than 0.9 are considered reliable for model prediction. Generally, the closer the value is to 1, the better the model fits the data [42].

2.4. Partitioning of Potential Suitable Areas

According to the results of MaxEnt, the suitability of *C. buqueti*'s distribution was divided into four levels: high-suitability area ($p \geq 0.66$), medium-suitability area ($0.33 \leq p < 0.66$), low-suitability area ($0.05 \leq p < 0.33$), and unsuitable area ($p < 0.05$). This classification was based on the method of assessing probabilities in the IPCC report to partition distribution values, using the suitability index P as the basis. Subsequently, the areas of different suitability zones were calculated using the Grid Calculation tool in ArcGIS 10.5.

2.5. Temporal and Spatial Changes in Suitable Habitat and Centroid

Using the coordinates of the grids in the model to calculate the average yielded the centroid, identifying the center point of *C. buqueti*'s distribution. The variation in this point reflected the geographical migration process of the target species. The SDM toolbox was employed to compute the centroid migration distance of *C. buqueti* within suitable areas under different time periods and climate scenarios. Subsequently, the spatiotemporal changes in the 2050s and 2070s, as well as the centroid variation in highly suitable habitats under three climate scenarios, were obtained.

3. Results

3.1. Model Performance and Validation

To assess the performance of MaxEnt, this study utilized the Receiver Operating Characteristic Curve (ROC), an independent threshold measure of model performance, indicating the model's ability to differentiate between presence and background data. This curve was employed to evaluate the performance of the MaxEnt model. Regarding the

Area Under the Curve (AUC) of the reconstructed model, as shown in Figure 1, the average AUC obtained from these repetitions was as high as 0.981, with a standard deviation of 0.001. According to the classification criteria mentioned earlier, this indicated excellent predictive performance of the model. AUC values consistently exceeding 0.9 suggested that the model possessed high predictive accuracy, rendering it suitable for predicting the potential distribution of *C. buqueti*.

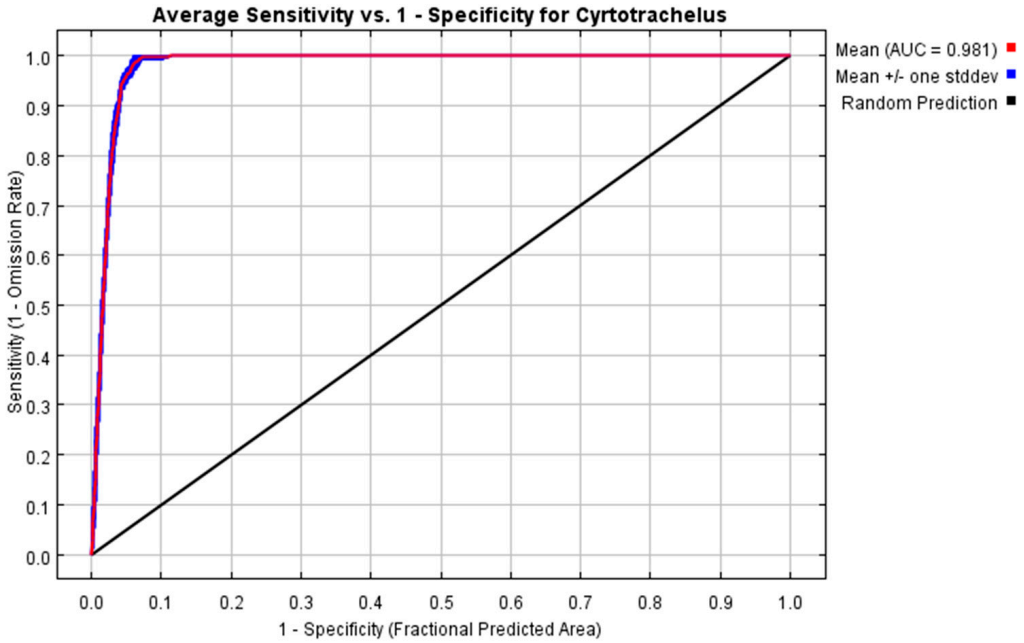

Figure 1. Receiver Operating Characteristic Curve and AUC result of Maxent modeling.

3.2. Key Environmental Variables and Response Curve Analysis

Table 2 shows the estimated relative contributions of key variables selected for the MaxEnt model. From the table, it was observed that the percentage contribution of the precipitation of the driest month (BIO 14) was the highest at 41.3%. The jackknife test, as shown in Figure 2, presented the average values obtained after ten repetitions. Among the five variables selected by MaxEnt (BIO 14, BIO 8, Elev, slope, and aspect), when used independently, BIO 14 exhibited the highest gain value. This aligned with the contribution results, indicating the latter as the most influential factor in shaping the distribution of the target species. The mean temperature of the wettest quarter (BIO 8) followed BIO 14 in terms of contribution, showing a similarly high gain value. The cumulative contribution of the top three variables—BIO 14, BIO 8, and Elev—was as high as 97.9%. Therefore, BIO 14, BIO 8, and Elev were identified as the primary environmental variables affecting the habitat suitability of *C. buqueti*, effectively reflecting the potential habitat conditions for this species.

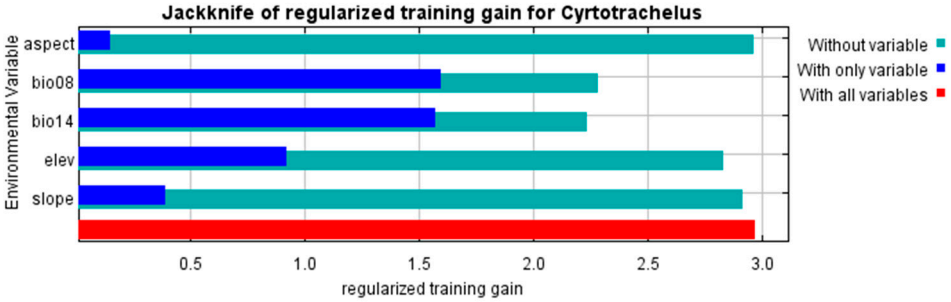

Figure 2. Importance of environmental variables to *C. buqueti* according to the jackknife test.

Table 2. Percent contribution (%) and permutation importance (%) of environmental variables in predicting the occurrence of *Cyrtotrachelus buqueti* (Guer) in the MaxEnt model.

Code	Percent Contribution/%
BIO 14 (precipitation of the driest month (mm))	41.3
BIO 8 (mean temperature of the wettest quarter (°C))	36.4
Elev (m)	20.2
Slope (°)	1.8
Aspect (°)	0.3

Based on the key environmental variables selected above, we produced response curve graphs for these variables (Figure 3). These curves illustrated how each environmental variable influenced MaxEnt predictions and how the predicted probability of occurrence changed with variations in each environmental variable. They reflected the dependency of the predicted suitability on the selected variables and the dependency arising from the correlation between the selected variables and other variables. When the precipitation of the driest month (BIO 14) reached 17.22 mm, its output value peaked at 0.69 (Figure 3a). This indicated that the probability of *C. buqueti* presence was highest when this precipitation level was reached. In terms of temperature, the mean temperature of the wettest quarter had the greatest impact on its distribution. As shown in Figure 3b, when this temperature reached 24.31 °C, it was most suitable for the target species' survival, with an output value of 0.63. Regarding elevation's influence, it can be inferred from Figure 3c that the peak occurred when *C. buqueti* was at an altitude of 451.8 m, with an output value of 0.66. The response curves of these three environmental factors exhibited distinct peaks, representing the most suitable conditions. In contrast, the variations in the impact of the remaining variables on its distribution appeared more complex. From Figure 3d, it can be observed that the slope curve showed a rapid rise before 4.00°. After 4.83°, the increase became increasingly gradual. The optimal slope for the distribution of *C. buqueti* was reached at 16.71°, with an output value of 0.77. Subsequently, the output value began to decrease. When the slope continued to increase to 22.7°, the output value had already dropped to 0.53. It was worth noting that although there was no occurrence of a slope more suitable for the survival of the target species than 16.71°, a second small peak appeared at 25.90°. Its output value was 0.68. Regarding the aspect, three peaks appeared at 105.04°, 302.53°, and 357.44°, respectively. The output values for these peaks were 0.65, 0.56, and 0.48, respectively. Based on their output values, the optimal aspect was determined to be 105.04°.

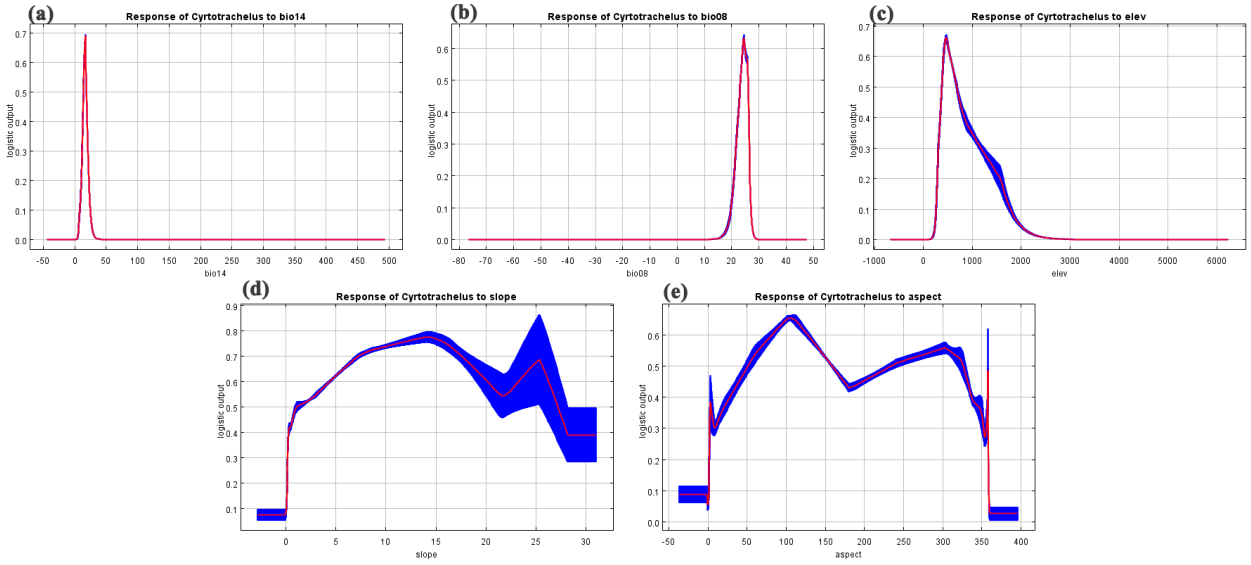

Figure 3. Response curves of the environmental variables that contributed most to the MaxEnt models. (**a**) Precipitation of the driest month (mm) (Bio 14). (**b**) Mean temperature of the wettest quarter (°C) (Bio 8). (**c**) Elev. (**d**) Slope. (**e**) Aspect.

3.3. Prediction and Variation of Potential Suitable Habitat for C. buqueti (Present/Future)

C. buqueti was predominantly distributed in southern China, particularly in the area of high suitability (Figure 4). Table 3 displayed the distribution area of *C. buqueti* under various current and future climate scenarios, calculated from raster counts. Based on the table, the areas of high, medium, and low suitability under the current conditions were 4.35 × 10^4 km^2, 32.41 × 10^4 km^2, and 55.35 × 10^4 km^2, respectively. These regions mainly included provinces such as Chongqing, Guizhou, Yunnan, Sichuan, Guangxi, Shaanxi, Hubei, Hainan, Taiwan, and Henan. For future distribution predictions, this study primarily investigated the distribution trends of *C. buqueti* in two future periods, i.e., 2050s and 2070s, and under three scenarios, namely, SSP1-2.6, SSP3-7.0, and SSP5-8.5. For future changes, as shown in Table 3, the distribution areas of high, medium, and low suitability demonstrated varying degrees of expansion compared to contemporary areas, regardless of the time period and climate scenario. It was reassuring that the expansion trend of *C. buqueti* was not significant. However, the expansion of the area of high suitability was more pronounced compared to other periods. Under the SSP3-7.0 scenario in the 2050s, the expansion of the area of high suitability for this pest was the most extensive, reaching 1.19%. The area of high suitability for *C. buqueti* warranted particular attention.

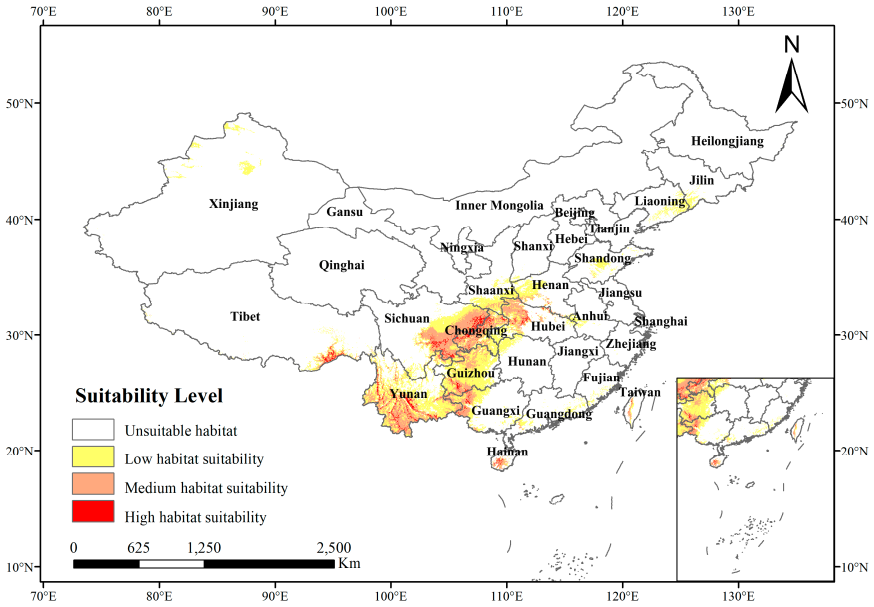

Figure 4. Current suitable climatic distribution of *C. buqueti* in China. The probability of *C. buqueti* is shown by the color scale in the area. Red indicates a highly suitable area with a probability of higher than 0.66, orange indicates a moderately suitable area with a probability of 0.33–0.66, yellow indicates a poorly suitable area with a probability ranging from 0.05–0.33, and white represents unsuitable areas.

Table 3. Prediction of the suitable areas for *C. buqueti* under current and future climatic conditions.

Decade	Scenarios	Predicted Area (10^4 km^2)			Comparison to the Current Distribution (%)		
		High-Suitability Area	Medium-Suitability Area	Low-Suitability Area	High-Suitability Area	Medium-Suitability Area	Low-Suitability Area
Current		4.35	32.41	55.35			
2050s	SSP1-2.6	8.60	35.41	68.96	0.98	0.09	0.25
	SSP3-7.0	9.52	32.42	56.17	1.19	0.00	0.01
	SSP5-8.5	6.23	35.29	69.75	0.43	0.09	0.26
2070s	SSP1-2.6	7.10	33.86	64.18	0.63	0.04	0.16
	SSP3-7.0	9.39	33.99	69.77	1.16	0.05	0.26
	SSP5-8.5	5.84	28.99	66.61	0.34	−0.11	0.20

3.4. Spatiotemporal and Centroid Changes of the High-Suitability Habitat

Figure 5 depicts the changing trends in the geographical distribution of *C. buqueti* under different future climate scenarios. Considering the centroid displacement changes for this insect (Figure 6), the centroid was primarily distributed in two provinces, namely, Yunnan and Guizhou. Under all three climate scenarios, centroids started their movement from Yunnan Province. For the SSP1-2.6 (Figure 5a,d) scenario, the centroid of *C. buqueti* shifted from Yunnan Province to Guizhou Province between the 2030s and 2070s, with relatively minor movement within Guizhou. This trend was similar under the SSP3-7.0 (Figure 5b,e) scenario, with even less movement observed within Guizhou. Notably, under the SSP5-8.5 (Figure 5c,f) scenario, *C. buqueti*'s movement was most pronounced, with the centroid shifting from the northeastern part of Yunnan Province to the western part of Guizhou Province during the same period. Overall, the movement direction of *C. buqueti* showed a tendency to shift southward with changing climates.

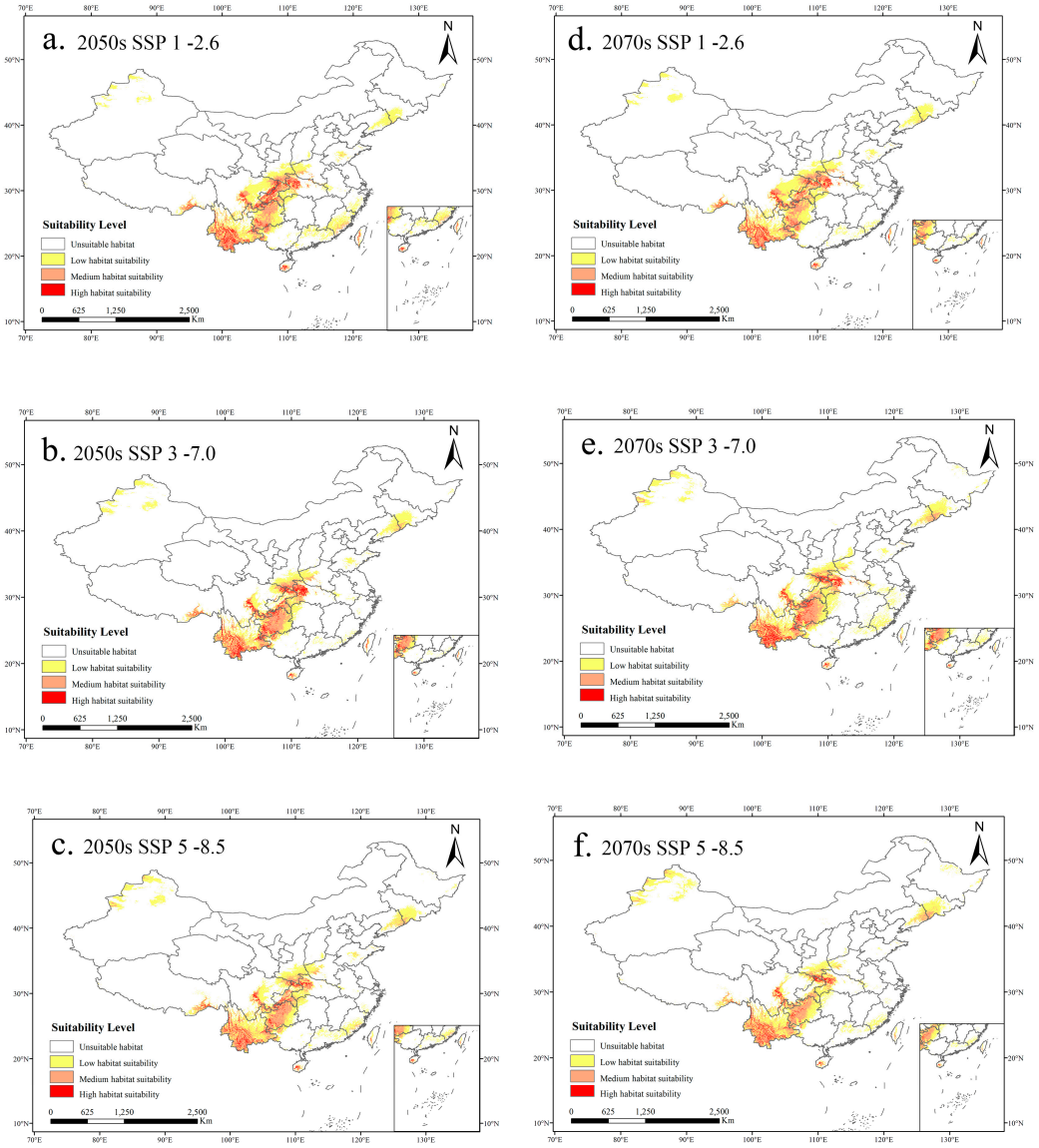

Figure 5. Potential distribution of suitable areas of *C. buqueti* under different climate change scenarios in China. The probability of *C. buqueti* is shown by the color scale in the area. Red indicates a highly suitable area with a probability of higher than 0.66, orange indicates a moderately suitable area with a probability of 0.33–0.66, yellow indicates a poorly suitable area with a probability ranging from 0.05–0.33, and white represents unsuitable areas.

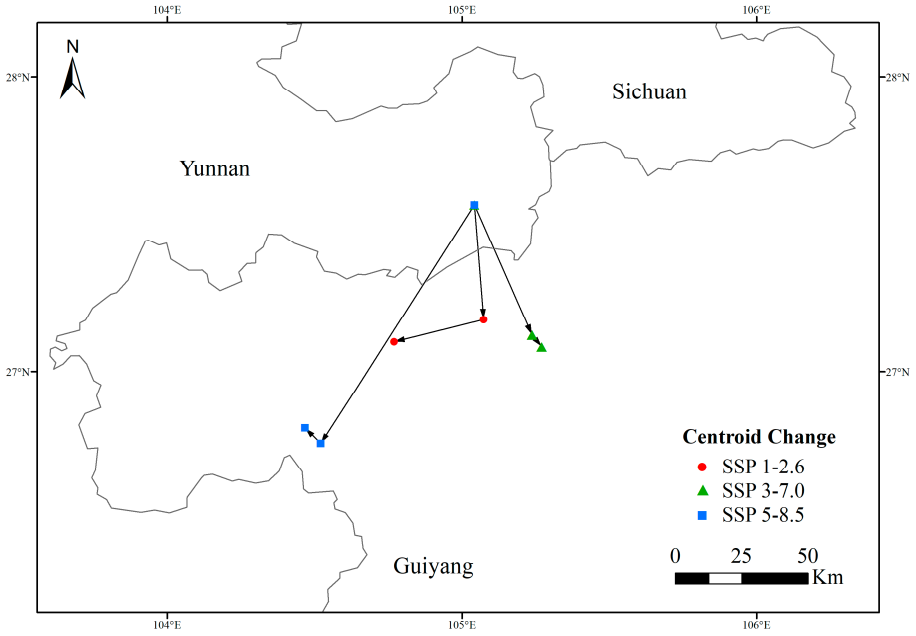

Figure 6. Centroid variation diagram of *C. buqueti*.

4. Discussion

MaxEnt can infer the distribution of target species and their tolerance to environmental conditions based on occurrence data. It allows researchers to fit models of arbitrary complexity. Studies have also shown that if the target species may occur across a wide range of environmental conditions, MaxEnt is preferred [43]. The predicted distribution conditions of *C. buqueti* in this study precisely match the requirements of the MaxEnt model. Combined with the advantages mentioned earlier, this model is deemed optimal for predictions. However, there may be instances during the model's usage where thorough checks are not conducted or the correct interpretation is not applied. Predictive work may commence without fully considering the limitations of the model or its assumptions. Considering the complexity of MaxEnt, this is a factor worth contemplating. By default, the fitting process utilizes all provided features and relatively low regularization multipliers, leading to over-parameterization. However, studies have shown that adjusting regularization parameters for specific species can optimize model complexity. Moreover, constraining the feature classes used during model fitting can generate more interpretable and transferable models [44]. In addition, overfitting can be quantified, and overly complex models can be detected by obtaining independent evaluation data. Adjusting program settings can also help determine the optimal model complexity settings [45]. In this study, these uncertainties have been largely mitigated through appropriate processing. It is worth noting that this study solely utilized the MAXENT model for modeling, and the use of a single predictive model also has certain limitations. In the future, we will consider integrating other prediction models to achieve more accurate forecasts.

According to the modeling results, currently, *C. buqueti* is distributed in Chongqing, Guizhou, Yunnan, Sichuan, Guangxi, Shaanxi, Hubei, Hainan, Taiwan, Tibet, Guangdong, Shandong, Liaoning, Xinjiang, Henan, and Fujian (Figure 4). This is broadly consistent with other relevant literature on its current distribution [10,46]. The results also indicate that the pest is primarily concentrated in Chongqing, Guizhou, and Yunnan. These three provinces are mainly influenced by a subtropical monsoon climate, characterized by hot and rainy summers and mild and dry winters. The overall climate features a rainy and warm period. This can also explain the condition of BIO 8, as identified in this study. BIO 8 describes the mean temperature of the wettest quarter. In the context of the monsoon climate's rainy and warm characteristics, increased precipitation leads to humid conditions, accompanied by rising temperatures. Therefore, the simultaneous variation in humidity and temperature

meets the survival requirements of *C. buqueti*. There are also studies suggesting that *C. buqueti* is suitable for distribution at altitudes around 400 m. For instance, in the most severely affected region in Sichuan Province, China (103.6 E, 29.2 N), the altitude is around 400 m [3]. This also corresponds to the findings of this study. The influence of Elev, slope, and aspect on the distribution of *C. buqueti* may be attributed to the habitat conditions of bamboo.

In recent years, research on *C. buqueti* has mainly focused on its biological characteristics and scientific control measures [10]. As with most harmful insects, the primary strategy for combating pests has been chemical control, mainly due to reasons such as cost and convenience. However, the overuse of chemical pesticides poses serious risks to the environment and biodiversity [47]. This is clearly undesirable. Research has shown that the prudent protection and utilization of natural enemies such as spiders, ants, wasps, birds, frogs, toads, *Notobitus meleagris* (predatory natural enemies), and *Telenomus gifuensis* Ashmead (parasitic natural enemy) can, to some extent, control *C. buqueti*. By combining the predicted future Suitable Area distribution in this article, dynamic monitoring of areas prone to pest infestation can be conducted. Based on this, these natural enemies can be released in a scientifically informed manner. This approach can significantly enhance targeted pest control efforts [48].

Combining three terrain factors and nineteen bioclimatic variables, the MaxEnt model was employed for modeling. This was utilized to predict the current and future distribution of *C. buqueti* under different climate scenarios, followed by a ranking assessment. The aim was to explore the impact of various factors on its distribution and identify key environmental variables. This study offers a new perspective regarding the control of *C. buqueti*. By predicting its future geographical distribution, it provides a reference for areas where occurrences have not yet happened or may occur in the future.

5. Conclusions

In this study, the MaxEnt model successfully simulated the potential geographical distribution of *C. buqueti* under current and future conditions (2050s and 2070s) across three climate change scenarios (SSP1-2.6, SSP3-7.0, and SSP5-8.5). Under current climate conditions, the insect is distributed in southern regions such as Chongqing, Guizhou, Yunnan, Sichuan, Guangxi, Shaanxi, Hubei, Hainan, and Taiwan. Among them, Chongqing, Guizhou, and Yunnan are the main distribution areas of high suitability. The most significant factors (thresholds) influencing its distribution are precipitation, followed by temperature, including precipitation of the driest month (17.22 mm) and mean temperature of the wettest quarter (24.31 °C). This study aims to provide theoretical references for the future control of *C. buqueti* from the perspective of geographical distribution.

Supplementary Materials: The following supporting information can be downloaded at: https://www.mdpi.com/article/10.3390/f15061049/s1, Table S1: Model Parameter Setting.

Author Contributions: Conceptualization, C.F. and Z.W.; Data curation, Y.P.; Formal analysis, Z.W.; Investigation, Y.P.; Methodology, C.F. and Z.W.; Resources, Z.Z.; Software, Y.P. and Z.Z.; Writing—original draft, C.F.; Writing—review and editing, Z.W. and Z.Z. All authors have read and agreed to the published version of the manuscript.

Funding: This research was supported by the Sichuan Province Key Lab for Bamboo Pest Control and Resource Development (ZLKF202309 and ZLKF202103), Sichuan Provincial Department of Science and Technology (2022NSFSC0986), Fundamental Research Funds of China West Normal University (20A007, 20E051, 21E040 and 22kA011).

Data Availability Statement: The data supporting the results are available in a public repository at: GBIF.org (03 April 2024) GBIF Occurrence Download https://www.gbif.org/zh/occurrence/download?taxon_key=1170493 (accessed on 3 April 2024) Zhiling Wang (2024). *Cyrtotrachelus buqueti* Occurrence data. figshare. Dataset. https://figshare.com/articles/dataset/_i_Cyrtotrachelus_buqueti_i_Occurrence_data/25559085 (accessed on 7 April 2024).

Conflicts of Interest: The authors declare no conflicts of interest.

References

1. Ding-Ze, M.; Qing-Huai, L.; Min, S.; Wei, W. Extraction and identification of cuticular semiochemical components of *Cyrtotrachelus buqueti* Guerin-Meneville (*Coleoptera: Curculionidae*). *Acta Entomol. Sin.* **2012**, *55*, 291–302.
2. Ruiting, J.; Cuihua, X.; Junhua, X.; Ying, X.; Xingzhen, J.; Yuezhong, L. *Cyrtotrachelus buqueti* in Shanghai. *For. Pest Dis.* **2005**, *24*, 7–9. [CrossRef]
3. Wang, J.; Wang, F.; Wang, R.; Zhang, J.; Zhao, X.; Yang, H.; Yang, W.; Yang, C.; Wang, Z.; Li, A. Modeling the effects of bioclimatic characteristics and distribution on the occurrence of *Cyrtotrachelus buqueti* in the Sichuan Basin. *Glob. Ecol. Conserv.* **2019**, *17*, e540. [CrossRef]
4. Yaojun, Y.; Shufang, W.; Bow, G.; Liu, C.; Ying, M.; Hong, Q. Relationships among *Cyrtotrachelus buqueti* larval density and worm hole number and bamboo shoot damage degree. *Chin. J. Appl. Ecol.* **2009**, *20*, 1980–1985.
5. Jian, W.; Fuyun, L.; Chunxia, X.; Hongjie, W. Numerical analysis and experimental results of output performance for large mode area Yb-doped double-clad fiber lasers. In *Optoelectronic Devices and Integration*; SPIE: Bellingham, WA, USA, 2005; pp. 540–544.
6. Liping, L.; Yaojun, Y.; Wencong, L.; Hong, L.; Chun, F.U. A Study of the Dynamic Changes of Volatiles on the Body Surface of *Cyrtotrachelus buqueti* Adults. *J. Sichuan For. Sci. Technol.* **2020**, *41*, 108–117. [CrossRef]
7. Yuan-feng, P.U.; Xue-li, Z.; Hua, Y.; Yan-lin, L. Feeding Behavior of *Cyrtotrachelus buqueti*. *J. Sichuan For. Sci. Technol.* **2018**, *39*, 100–104. [CrossRef]
8. Chen, F.Z. Preliminary Investigation on Cyrtotrachelus longimanus in Sinocalamus affinisof Muchuan County. *J. Leshan Teach. Coll.* **2002**.
9. Fuxiang, D.; Qing, G.; Wencong, L.; Haibo, Y.; Yaojun, Y. The Ultrastructure of Respiratory System of *Cyrtotrachelus buqueti* Guer. *J. Sichuan For. Sci. Technol.* **2020**, *41*, 100–107. [CrossRef]
10. Fu, C.; Long, W.; Luo, C.; Nong, X.; Xiao, X.; Liao, H.; Li, Y.; Chen, Y.; Yu, J.; Cheng, S.; et al. Chromosome-Level Genome Assembly of *Cyrtotrachelus buqueti* and Mining of Its Specific Genes. *Front. Ecol. Evol.* **2021**, *9*, 729100. [CrossRef]
11. Yangh, Y.; Wang, S.; Mou, C. A Preliminary Report on Investigation of Bamboo Diseases and Pests in Leshan City, Sichuan Province. *Prot. Bamboo* **2008**. [CrossRef]
12. Xuewen, N. Preliminary Report on Experiment of Biological Features of *Cyrtotrachelus buqueti* and Its Prevention and Control. *For. Inventory Plan.* **2010**, *35*, 99–102. [CrossRef]
13. Li, X.; Zheng, Y. Functional characteristics of the rigid elytra in a bamboo weevil beetle *Cyrtotrachelus buqueti*. *Iet Nanobiotechnol.* **2022**, *16*, 273–283. [CrossRef]
14. Li, X.; Guo, C.; Li, L. Functional morphology and structural characteristics of the hind wings of the bamboo weevil *Cyrtotrachelus buqueti* (*Coleoptera*, *Curculionidae*). *Anim. Cells Syst.* **2019**, *23*, 143–153. [CrossRef]
15. Li, L.; Guo, C.; Liu, L.; Liu, L.; Hu, Z.; Guo, H.; He, S. Design optimization of lightweight structures inspired by the rostrum in *Cyrtotrachelus buqueti* Guer (*Coleoptera: Curculionidae*). *Mater. Res. Express* **2022**, *9*, 115009. [CrossRef]
16. Li, L.; Guo, C.; Xu, S.; Ma, Y.; Yu, Z. Nanoindentation Properties and Finite Element Analysis of the Rostrum of *Cyrtotrachelus buqueti* Guer (*Coleoptera: Curculionidae*). *Microsc. Microanal.* **2019**, *25*, 786–797. [CrossRef]
17. Zhang, Z.; Rao, F.; Wang, Y. Morphological, Chemical, and Physical–Mechanical Properties of a Clumping Bamboo (*Thyrsostachys oliveri*) for Construction Applications. *Polymer* **2022**, *14*, 3681. [CrossRef]
18. Ramakrishnan, M.; Yrjälä, K.; Vinod, K.; Sharma, A.; Cho, J.; Satheesh, V.; Mingbing, Z. Genetics and genomics of moso bamboo (*Phyllostachys edulis*): Current status, future challenges, and biotechnological opportunities toward a sustainable bamboo industry. *Food Energy Secur.* **2020**, *9*, e229. [CrossRef]
19. Sánchez-Matiz, J.J.; Díaz-Ariza, L.A. Glomeromycota associations with bamboos (Bambusoideae) worldwide, a qualitative systematic review of a promising symbiosis. *PeerJ* **2023**, *11*, e16151. [CrossRef]
20. Srivaro, S.; Rattanarat, J.; Noothong, P. Comparison of the anatomical characteristics and physical and mechanical properties of oil palm and bamboo trunks. *J. Wood Sci.* **2018**, *64*, 186–192. [CrossRef]
21. Singh, L.; Sridharan, S.; Thul, S.; Kokate, P.; Kumar, P.; Kumar, S.; Kumar, R. Eco-rejuvenation of degraded land by microbe assisted bamboo plantation. *Ind. Crop. Prod.* **2020**, *155*, 112795. [CrossRef]
22. Lieurance, D.; Cooper, A.; Young, A.L.; Gordon, D.R.; Flory, S.L. Running bamboo species pose a greater invasion risk than clumping bamboo species in the continental United States. *J. Nat. Conserv.* **2018**, *43*, 39–45. [CrossRef]
23. Singh, A.; Singh, J.S. Biomass, net primary production and impact of bamboo plantation on soil redevelopment in a dry tropical region. *For. Ecol. Manag. For. Ecol Manag.* **1999**, *119*, 195–207. [CrossRef]
24. Padgurschi, M.C.G.; Vieira, S.A.; Stefani, E.J.F.; Nardoto, G.B.; Joly, C.A. Nitrogen input by bamboos in neotropical forest: A new perspective. *PeerJ* **2018**, *6*, e6024. [CrossRef]
25. Christanty, L.; Kimmins, J.P.; Mailly, D. 'Without bamboo, the land dies': A conceptual model of the biogeochemical role of bamboo in an Indonesian agroforestry system. *For. Ecol. Manag.* **1997**, *91*, 83–91. [CrossRef]
26. Luo, C.; Li, Y.; Chen, Y.; Fu, C.; Nong, X.; Yang, Y. Degradation of bamboo lignocellulose by bamboo snout beetle *Cyrtotrachelus buqueti* in vivo and vitro: Efficiency and mechanism. *Biotechnol. Biofuels* **2019**, *12*, 75. [CrossRef]
27. Luo, C.; Li, Y.; Liao, H.; Yang, Y. De novo transcriptome assembly of the bamboo snout beetle *Cyrtotrachelus buqueti* reveals ability to degrade lignocellulose of bamboo feedstock. *Biotechnol. Biofuels* **2018**, *11*, 292. [CrossRef]
28. Gao, S.S. Study on Culm-form Structure and Physical and Mechanical Properties of Four Kinds of Big Sympodial Bamboo. Master's Thesis, Nanjing Forestry University, Nanjing, China, 2011.

29. Elith, J.; Leathwick, J. Species Distribution Models: Ecological Explanation and Prediction Across Space and Time. *Annu. Rev. Ecol. Evol. Syst.* **2009**, *40*, 677–697. [CrossRef]
30. Lembrechts, J.J.; Nijs, I.; Lenoir, J. Incorporating microclimate into species distribution models. *Ecography* **2018**, *42*. [CrossRef]
31. Candela, L.; Castelli, D.; Coro, G.; Pagano, P.; Sinibaldi, F. Species distribution modeling in the cloud. *Concurr. Comput. Pract. Exp.* **2016**, *28*, 1056–1079. [CrossRef]
32. Phillips, S.; Anderson, R.; Schapire, R.; Phillips, S.J.; Anderson, R.P.; Schapire, R.E. Maximum entropy modeling of species geographic distribution. *Ecol. Model.* **2013**, *190*, 231–259. [CrossRef]
33. Glor, R.; Warren, D. Testing ecological explanations for biogeographic boundaries. *Evol. Int. J. Org. Evol.* **2010**, *65*, 673–683. [CrossRef]
34. Cardoso-Leite, R.; Vilarinho, A.; Novaes, M.; Tonetto, A.; Vilardi, G.; Guillermo-Ferreira, R. Recent and future environmental suitability to dengue fever in Brazil using species distribution model. *R. Soc. Trop. Med. Hyg.* **2014**, *108*, 99–104. [CrossRef]
35. Warren, D.L.; Wright, A.N.; Seifert, S.N.; Shaffer, H.B. Incorporating model complexity and spatial sampling bias into ecological niche models of climate change risks faced by 90 California vertebrate species of concern. *Divers. Distrib.* **2014**, *20*, 334–343. [CrossRef]
36. Rodda, G.H.; Jarnevich, C.S.; Reed, R.N. Challenges in Identifying Sites Climatically Matched to the Native Ranges of Animal Invaders. *PLoS ONE* **2011**, *6*, e14670. [CrossRef]
37. Bradie, J.; Leung, B. A quantitative synthesis of the importance of variables used in MaxEnt species distribution models. *J. Biogeogr.* **2017**, *44*, 1344–1361. [CrossRef]
38. Losada, M.; Holik, F.; Massri, C.; Plastino, A. Solutions for the MaxEnt problem with symmetry constraints. *Quantum Inf. Process.* **2019**, *18*, 293. [CrossRef]
39. Mazzoni, D.S. Distribution Modelling by MaxEnt: From Black Box to Flexible Toolbox. Ph.D. Thesis, University of Oslo, Oslo, Norway, 2016.
40. Li, Q. Modeling and mapping the current and future distribution of *Pseudomonas syringae* pv. actinidiae under climate change in China v1. *PLoS ONE* **2017**.
41. Dirick, L.; Claeskens, G.; Baesens, B. An Akaike information criterion for multiple event mixture cure models. *Eur. J. Oper. Res.* **2015**, *241*, 449–457. [CrossRef]
42. Wang, Z.; Xu, D.; Liao, W.; Xu, Y.; Zhuo, Z. Predicting the Current and Future Distributions of *Frankliniella occidentalis* (Pergande) Based on the MaxEnt Species Distribution Model. *Insects* **2023**, *14*, 458. [CrossRef]
43. Wang, L.; Jackson, D. Effects of sample size, data quality, and species response in environmental space on modeling species distributions. *Landsc. Ecol.* **2023**, *38*, 1–23. [CrossRef]
44. Low, B.W.; Zeng, Y.; Tan, H.H.; Yeo, D.C.J. Predictor complexity and feature selection affect Maxent model transferability: Evidence from global freshwater invasive species. *Divers. Distrib.* **2021**, *27*, 497–511. [CrossRef]
45. Radosavljevic, A.; Anderson, R.P. Making better Maxent models of species distributions: Complexity, overfitting and evaluation. *J. Biogeogr.* **2014**, *41*, 629–643. [CrossRef]
46. Yang, H.; Liu, Y.; Tao, Y.; Yang, W.; Yang, C.; Zhang, J.; Qian, L.; Liu, H.; Wang, Z. Bioinformatic and biochemical analysis of the key binding sites of the pheromone binding protein of *Cyrtotrachelus buqueti* Guerin-Meneville (Coleoptera: Curculionidea). *PeerJ* **2019**, *7*, e7818. [CrossRef]
47. Liu, L.; Wang, F.; Yang, W.; Yang, H.; Huang, Q.; Yang, C.; Hui, W. Molecular and Functional Characterization of Pheromone Binding Protein 2 from *Cyrtotrachelus buqueti* (*Coleoptera: Curculionidae*). *Int. J. Mol. Sci.* **2023**, *24*, 16925. [CrossRef]
48. Zhan, Z.; He, X.; Zhang, L.; Zheng, H.; Lin, J. Integrated control technology of main pests of green bamboo. *For. By-Prod. Spec. China* **2017**, *6*, 61–64. [CrossRef]